Plasma gelsolin protects HIV-1 gp120-Induced neuronal injury via voltage-gated K+ channel Kv2.1

Han Liu[1,2], **Jianuo Liu**[2], **Shangdong Liang**[1,*], and **Huangui Xiong**[2,*]

[1]Department of Physiology, College of Basic Medical Sciences, Nanchang University, Nanchang, Jiangxi, People Republic of China

[2]Department of Pharmacology and Experimental Neuroscience, University of Nebraska Medical Center, Omaha, NE 68198-5880

Abstract

Plasma gelsolin (pGSN), a secreted form of gelsolin, is constitutively expressed throughout the central nervous system (CNS). Neurons, astrocytes and oligodendrocytes are the major sources of pGSN in the CNS. It has been shown that levels of pGSN in cerebrospinal fluid (CSF) are decreased in several neurological conditions including HIV-1-associated neurocognitive disorders (HAND). Although there is no direct evidence that a decreased level of pGSN in CSF is causally related to the pathogenesis of neurological disorders, neural cells, if lacking pGSN, are more vulnerable to cell death. To understand how GSN levels relate to neuronal injury in HAND, we studied the effects of pGSN on HIV-1 gp120-activated outward K^+ currents in primary rat cortical neuronal cultures. Incubation of rat cortical neurons with gp120 enhanced the outward K^+ currents induced by voltage steps and resulted in neuronal apoptosis. Treatment with pGSN suppressed the gp120-induced increase of delayed rectifier current (I_K) and reduced vulnerability to gp120-induced neuronal apoptosis. Application of Guangxitoxin-1E (GxTx), a Kv2.1 specific channel inhibitor, inhibited gp120 enhancement of I_K and associated neuronal apoptosis, similar effects to pGSN. Western blot and PCR analysis revealed gp120 exposure to up-regulate Kv2.1 channel expression, which was also inhibited by treatment with pGSN. Taken together, these results indicate pGSN protects neurons by suppressing gp120 enhancement of I_K through Kv2.1 channels and reduction of pGSN in HIV-1-infected brain may contribute to HIV-1-associated neuropathy.

Keywords

Cortical neurons; Kv channels; HIV-1gp120; Neuronal injury; Plasma gelsolin; Neuroprotection

*Co-corresponding authors: Huangui Xiong, MD, PhD, Department of Pharmacology and Experimental Neuroscience, University of Nebraska Medical Center, Omaha, NE 68198-5880, Phone: 402-559-5140, Fax: 402-559-3744, hxiong@unmc.edu. Shangdong Liang, MD, PhD, Department of Physiology, College of Basic Medical Sciences, Nanchang University, Nanchang, Jiangxi, People Republic of China, Phone: 86-791-8636-0552, liangsd@hotmail.com.

Competing Interests: The authors have declared that no competing interests exist.

Introduction

With the advent of antiretroviral therapy (ART), the morbidity and mortality resulting from HIV-1 infection has been lessened. However, the incidence of HIV-1-associated neurocognitive disorders (HAND) continues and, due to the longer lifespans of treated patients, the prevalence may actually be increasing (Heaton et al., 2010; Kranick and Nath, 2012; McArthur and Smith, 2013; Mothobi and Brew, 2012). Although productive HIV-1 infection of neuronal cells has not been demonstrated, it is well accepted that neurons are affected by HIV-1 through indirect mechanisms (Kaul and Lipton, 2006b; Nath and Geiger, 1998; Xiong et al., 2000). These include the release of soluble neurotoxins from HIV-1-infected and immune competent mononuclear phagocytes (perivascular brain macrophage and microglia), leading to neuronal dysfunction and injury (Gendelman et al., 1998; Kaul and Lipton, 2006b). Such neurotoxic substances include, but not limited to, proinflammatory cytokines, chemokines, excitatory amino acids, and viral proteins (gp120 and *Tat*), which can injure or kill neurons. (Mattson et al., 2005). In particular, the envelope protein gp120 has been shown to be lethal to neurons in culture through alterations in signal transduction and excitotoxic influx of Ca^{2+} (Catani et al., 2000; Meucci and Miller, 1996; Muller et al., 1992). For these reasons we chose to use gp120 to further investigate the mechanisms underlying HAND pathogenesis in our cell culture model.

Gelsolin (GSN) is a Ca^{2+-}dependent multifunctional actin severing protein. This protein exists in two isoforms, cytoplasmic gelsolin (cGSN) and plasma gelsolin (pGSN) (Yin et al., 1984). Both isoforms are functionally similar and encoded by a single gene on chromosome 9 (Kwiatkowski et al., 1986; Kwiatkowski et al., 1988). In addition to its widely recognized function as a cytoplasmic regulator of actin organization, accumulating evidence suggests GSN activity prevents neuronal apoptosis in multiple ways (Harms et al., 2004), including through the facilitation of voltage-dependent Ca^{2+} channel (VDCC) and NMDA-channel rundown following exposure to excitotoxic stimuli, thereby reducing cytosolic Ca^{2+} overload (Endres et al., 1999; Furukawa et al., 1997). Of particular relevance here, proteomic studies have revealed decreased pGSN levels in the cerebrospinal fluid (CSF) of HIV-infected individuals with cognitive disturbance (Rozek et al., 2007). In addition, altered pGSN levels have been noted in other neurological conditions (Carro, 2010; Kulakowska et al., 2008; Peng et al., 2011), such that pGSN is being considered as a biomarker for certain neurodegenerative disorders (Bucki et al., 2008; Haverland et al., 2010; Peng et al., 2011). In general, GSN has been found neuroprotective and is now being considered as a potential treatment modality in several diseases characterized by neuronal injury (Bucki et al., 2008; Carro, 2010; Kulakowska et al., 2010; Kulakowska et al., 2008; Le et al., 2011; Meisel et al., 2006).

Research on programmed cell death has demonstrated the necessary contribution of K^+ channels in the process of apoptosis. Regardless of the diverse external and internal stimuli that trigger cell apoptosis, enhanced K^+ efflux has been shown to be an essential mediator of apoptotic cell shrinkage, downstream caspase activation, and DNA fragmentation (Remillard and Yuan, 2004). In previous experiments, our laboratory has confirmed the association of rat cortical neuron apoptosis and increased outward K^+ currents in models of HAND (Chen et al., 2011; Hu et al., 2009; Keblesh et al., 2009b). While several Kv channel subtypes have been implicated in cortical neuron apoptosis, including Kv2.1 (Pal et al., 2003), Kv1.1 (Hu et al., 2008), Kv3.4 (Pannaccione et al., 2007), Kv4.2, and Kv4.4 (Pieri et al., 2010), the specific subtype involved in HAND pathology and the mechanism underlying its dysfunction remains to be definitively characterized. Collectively, these observations lead us to investigate the protective potential of pGSN against gp120-induced neuronal injury and to determine the function of specific Kv channel subunits in this neuroprotective activity.

Results

pGSN protects against gp120-induced neuronal toxicity

Although the typical cells infected with HIV-1 in the CNS are not neurons (Anderson et al., 2002), viral envelope glycoprotein gp120 has been demonstrated to induce neuronal apoptosis in cell cultures (Meucci and Miller, 1996; Muller et al., 1992). Further, while pGSN has been shown to be protective against excitotoxic insults (Furukawa et al., 1997), it is detected at significantly lower levels in the CSF of HIV-1-infected individuals who exhibit neurocognitive disorder (Rozek et al., 2007; Wiederin et al., 2009). In light of these findings, we sought to determine the effect of pGSN on gp120-induced neuronal toxicity. First, rat cortical neuronal cultures were prepared and incubated for 24 h with varying concentrations of gp120 (0–1000 pM). Neuronal viability was then assessed by MTT assay and found to diminish significantly at gp120 concentrations above 250 pM (Fig. 1A). Given the nearly 40% loss of viability at concentrations of and greater than 500 pM, the concentration of 500pM was utilized in neurotoxicity experiments. Next, neuronal cultures were treated for 24 h with 500 pM gp120 and different concentrations of pGSN (0–2500 ng/ml). pGSN was found to be significantly protective against gp120-induced toxicity at a concentration of 2.5 μg/ml (Fig. 1B).

pGSN inhibits gp120-induced increases of outward K^+ current

Activation of neuronal Kv channels has been shown in several studies to be involved in neuronal dysfunction and apoptosis (Pal et al., 2006; Yu et al., 1997). In HIV-1 infection, secreted cellular and viral products can increase Kv channel activity, leading to neuronal dysfunction and cognitive deficits (Keblesh et al., 2009a). Specifically, previous experiments in our laboratory have demonstrated gp120 can induce apoptosis by enhancing 4-AP-sensitive I_A current via CXCR4-PKC signaling (Chen et al., 2011). Given the prominent role of Kv channels in mediating neuronal damage, coupled with the protective effects of pGSN against gp120-induced neurotoxicity observed here, we further sought to determine if the protection provided by pGSN occurs via alterations in Kv channel activity. First, rat cortical neuron cultures were prepared and treated with gp120 at concentrations of 50pM or 100pM for 24 h. Whole-cell outward K^+ currents were then recorded. As shown in Figure 2A, gp120 produced an increase of outward K^+ currents. Further analyses revealed that gp120 significantly ($p<0.01$) increased both instantaneous and steady-state outward K^+ currents at a concentration of 100 pM (Fig. 2B). Next, we examined effects of pGSN on its blockade of gp120 increase of neuronal outward K^+ currents. Neuronal cultures were treated for 24 h with either 100 pM gp120 alone or with gp120 (100pM) and different concentrations of pGSN (0, 5, 50, 500ng/ml). As expected, gp120 enhanced both instantaneous and steady-state outward K^+ currents (Fig. 3). Treatment with pGSN reduced gp120-associated increase of outward K^+ currents, with a significant ($p<0.01$) reduction of the steady-state outward K^+ current at a concentration of 500 ng/ml (Fig. 3B). Application of pGSN alone at concentrations of 5, 50 and 500ng/ml (data not shown) or heat-inactivated pGSN (500ng/ml, Fig. 3B) had no significant effects on gp120 increase of outward K^+ currents. These results indicate that pGSN inhibits gp120 enhancement of neuronal steady-state outward K^+ current.

pGSN inhibits gp120 enhancement of TEA-sensitive I_K, but not 4-AP-sensitive I_A

TEA-sensitive I_K and 4-AP-sensitive I_A are two common outward K^+ currents recorded in neuronal cells. Previous studies indicate certain outward K^+ currents may be more involved in apoptosis (Yu, 2003). In order to determine the specific outward K^+ currents enhanced by exposure to gp120 and attenuated by treatment with pGSN, whole-cell recordings were repeated in the presence of 4-AP (5 mM) or TEA (40 mM). As seen in Figure 4, gp120 (100pM) augmented both 4-AP-sensitive I_A and TEA-sensitive I_K (Fig. 4A), while only

TEA-sensitive I_K was suppressed with GSN treatment (Figs. 4A and 4C). Application of pGSN (500 ng/ml) alone did not affect the outward K^+ current amplitude or current density of either type.

pGSN attenuates gp120 enhancement of I_K via Kv2.1

The Kv channel subtypes reported to be most responsible for neuronal injury and apoptosis are Kv1 (Hu et al., 2008; Shen et al., 2009), Kv4 (Lei et al., 2010), and Kv2 (Pal et al., 2003). In neurons, Kv1.1 and Kv4.2 are the principal components of I_A, while Kv2.1 is responsible for I_K (Murakoshi and Trimmer, 1999). Given our immediate findings, we postulated Kv2.1 channels to be the predominant mediator of the neuroprotection provided by pGSN. To test this hypothesis, we utilized the Kv2.1-specific inhibitor, Guangxitoxin (GxTx) (Herrington, 2007; Lee et al., 2010). Control, gp120, and gp120+pGSN groups were again prepared as described above. During the recordings, I_K was isolated by the addition of 4-AP (5 mM) to the bath solution and its Kv2.1 contribution suppressed by application of GxTx (50 nM). The addition of GxTx to the control group suppressed nearly 40% of the I_K component (Fig. 5B), demonstrating the contribution of Kv2.1 channels to the delayed outward K^+ current in these neurons. More importantly, the previously observed enhancements in I_K induced by exposure to gp120 were absent in the presence of GxTx, indicating the increase was comprised of current through Kv2.1 channels (Fig. 5). Lastly, the gp120-enhanced I_K attenuated by co-incubation with GSN was not further inhibited by the addition of GxTx, allowing us to infer that both may affect I_K via modulation of Kv2.1 channel activity.

pGSN blocks gp120-induced shift in TEA sensitive I_K inactivation curve

Alterations in the current amplitudes of ion channels are generally related to one of three possible factors: regulation of channel expression, promotion of channel translocation, or modification of channel activation. To define the mechanism of gp120 enhancement of I_K and its inhibition by pGSN, we next investigated the impact of gp120 and pGSN on Kv channel activation and inactivation properties. Rat cortical neuron cultures were first prepared for whole-cell recordings as described previously. I_K current was then isolated for recording by the addition of 4-AP to the bath solution. To characterize the steady-state inactivation behavior of I_K, 400 ms pre-conditioning pulses were applied to step the membrane potential from −120 mV to + 40 mV in 10 mV increments, followed by a 200 ms pulse to fix the membrane potential at +40 mV. I–V curves were then plotted and fit using the Boltzmann equation ($I/I_{max}=1/\{1+\exp[(V-V1/2)/k]\}$) to yield the inactivation curve (Fig. 6A, 6B). Similarly, the activation curve was generated by applying 400 ms depolarizing pulses to step the membrane potential from 120 to +40 mV in 20 mV increments and fitting the I–V data using the Boltzmann equation ($G/G_{max}=1-1/\{1+\exp[(V-V1/2)]/k\}$ (Fig. 6A, 6B). Having established the I_K inactivation and activation tendencies under control conditions, cells were then perfused for 10 min with either gp120 (200 pM) or gp120 (200 pM) + pGSN (1000 ng/ml) and recorded using the identical protocol. Exposure to gp120 was found to result in a significant right-ward shift of the steady-state I_K inactivation curve and a slight left-ward shift of the activation curve, reflecting a greater open channel probability at a given voltage. Further, the gp120-induced depolarizing shift in the inactivation curve was attenuated with pGSN co-perfusion (Fig.6B, 6C).

Inhibition of gp120-induced Kv2.1 channel expression by pGSN

To further characterize the mechanism of gp120-enhanced I_K and its reduction by GSN, we next examined alterations in Kv channel expression related to exposure to gp120 and pGSN. Rat cortical neurons were first incubated for 24 h with gp120 (500 pM), pGSN (2500 ng/ml), or gp120 and pGSN combined. The mRNA and protein levels of the Kv channels

responsible for outward K+ current in neurons, Kv1.1, Kv2.1, and Kv4.2, were then assessed by RT-PCR and Western blot. As expected, application of pGSN alone did not affect Kv channel mRNA expression. In comparison to control, exposure to gp120 increased the mRNA expression of all three channel subtypes, with Kv1.1 mRNA expression reaching statistical significance (Fig. 7A). Consistent with our electrophysiological findings, co-incubation with pGSN attenuated gp120-enhanced expression of Kv2.1 channel mRNA, but did not affect the elevated expression of Kv1.1 and Kv4.2 mRNA (Fig. 7A). Similarly, channel protein levels were unaffected by the application of pGSN alone, but were significantly increased for all three Kv channel subtypes in the gp120 exposed group (Fig. 7B). Again in agreement with our electrophysiological studies, co-incubation with pGSN was found to prevent gp120-induced elevation in Kv2.1 protein level, without inhibiting similar increases in the amount Kv1.1 and Kv4.2 proteins (Fig. 7B).

pGSN protects against gp120-induced neuronal damage via Kv2.1

Thus far, we have demonstrated pGSN treatment can mitigate gp120-induced loss of neuronal viability, while at the same time preventing the alterations in I_K (in)activation properties and Kv2.1 channel expression that underlie gp120 enhancement of I_K. In order to establish the involvement of Kv2.1 in gp120-associated neuronal injury and the neuroprotective activity of pGSN, we next performed studies on neuronal apoptosis and viability using gp120, pGSN, and the Kv2.1-specific inhibitor GxTx. First, rat cortical neuron cultures were incubated for 24 h with gp120 (500 pM), pGSN (2500 ng/ml), GxTx (12.5 or 25 nM), gp120 + pGSN, or gp120 + GxTx. Neuronal apoptosis was then assessed by TUNEL stain and neuronal viability by MTT assay. In comparison to control, neuronal viability was reduced by 33% in cultures incubated with gp120 (500 pM), while co-incubation treatment with pGSN (2500 ng/ml), GxTx (12.5 nM), or GxTx (25 nM) restored neuronal viability to 88.5%, 79.0%, and 83.0%, respectively (Fig. 8A). Similarily, exposure to gp120 resulted in a 5-fold increase in neuronal apoptosis, which was attenuated by GSN and GxTx in a dose-dependent manner (Fig. 8B).

Discussion

The consensus view regarding the pathogenesis of HAND centers around the secretion of neurotoxic substances from HIV-1-infected and immune activated brain mononuclear phagocytes (blood borne macrophages and microglia), including viral products such as gp120, causing neuronal dysfunction and apoptosis (Kaul et al., 2001; Kaul and Lipton, 2006a; Lipton and Gendelman, 1995; Nath et al., 2000). Given the requirement for K^+ efflux in processes of programmed cell death (Remillard and Yuan, 2004), our recent research has focused on the role of Kv channelopathies in HAND pathology (Chen et al., 2011; Gelman et al., 2004; Hu et al., 2009; Keblesh et al., 2009b). Based on research demonstrating the protective effect of GSN against Ca^{2+}-mediated excitotoxicity (Endres et al., 1999; Furukawa et al., 1997), combined with proteomic studies indicating the level of pGSN is decreased in the CSF of HIV-infected individuals with cognitive impairment (Rozek et al., 2007), here we delve into the connection between gp120, pGSN, and Kv channels. Presently we show two novel findings: first, the induction of neuronal injury by HIV-1 envelope protein gp120 entails enhanced I_K through Kv2.1 channels, and second, pGSN provides neuroprotection against gp120 by preventing the modification of channel expression and inactivation properties underlying I_K enhancement.

Previous research into the pathways of HAND neuropathogenesis has focused primarily on infected and/or activated mononuclear phagocyte releasing neurotoxins including, but not limited to, arachidonic acid, platelet-activation factor, free radicals, glutamate, quinolinate, cysteine, cytokines, amines and viral proteins (Tat and gp120). Although neurons do not

express CD4 receptor, a principal receptor for HIV-1 entry into host cells, they do express the chemokine and HIV-1 infection co-receptors CXCR4 and CCR5. Along with NMDA receptors, these receptors can be pathologically activated by aforementioned neurotoxins and viral products such as gp120, leading to alterations in signal transduction, excitotoxic influx of Ca^{2+}, neuronal dysfunction, and eventual apoptosis (Catani et al., 2000; Meucci and Miller, 1996; Muller et al., 1992). While the process of apoptosis is now generally accepted to involve excess K^+ efflux regardless of cell type or initiating stimuli (Remillard and Yuan, 2004; Yu, 2003), reports of Kv channel contribution to gp120-related neuronal damage are rare. In a previous publication, our data suggested gp120 may induce caspase-3 dependent neuronal apoptosis by enhancing I_A via CXCR4-PKC signaling (Chen et al., 2011). Results from the present experiments indicate gp120 exposure also leads to amplification of an I_K current (Fig. 4), which was found to be susceptible to Kv2.1-specific inhibition (Fig. 5), by provoking a depolarizing shift in I_K channel inactivation properties (Fig. 6) and an upregulation of Kv2.1 channel expression (Fig. 7). Furthermore, the significance of this increased Kv2.1 channel activity was demonstrated by MTT assay and TUNEL staining assessments of neuronal health, which established that gp120-induced neuronal damage could be alleviated by Kv2.1-specific inhibition (Fig. 8). These findings are consistent with research on hippocampal neurons demonstrating upregulation of Kv2.1 to be essential to the induction of apoptosis under conditions of excess glutamate, the natural ligand of NMDAR (Shen et al., 2009). In a similar experiment, glutamate was found to act through NMDAR to induce dephosphorylation of Kv2.1 channels and thereby alter channel function (Misonou et al., 2004). While HIV-1 infection of the CNS is associated with excess glutamate release and impaired uptake (Potter et al., 2013), gp120 is also known to trigger NMDAR-mediated neuronal death and thus may initiate similar apoptotic cascades (Potter et al., 2013; Wu et al., 1996).

Neuronal cell loss is a common feature of many neurodegenerative diseases. In order to better understand the cellular milieu in which this occurs and identify practical diagnostic markers, proteomic studies of CSF and plasma have been undertaken for numerous conditions including HAND. Proteomic analysis revealed that pGSN was diminished in the CNS across varied conditions characterized by neuronal injury or dysfunction, including Alzheimer's disease (Carro, 2010), multiple sclerosis (Kulakowska et al., 2008), and epilepsy (Peng et al., 2011). In HAND, pGSN is decreased in the CSF (Rozek et al., 2007) and elevated in plasma (Wiederin et al., 2009). Given the increased permeability of the blood brain barrier (BBB) associated with HIV-1 infection, the depletion of pGSN in the CSF may have significance for neuronal health and function, while the plasma abundance could be used as a diagnostic indicator (Haverland et al., 2010). It is important to note however, there are two isoforms of GSN, pGSN and cGSN, which may have different roles and be present in different concentrations (Pottiez et al., 2010). HIV-infected macrophage have been found to secrete pGSN (Jagadish et al., 2012), which has been shown to be involved in further recruitment of macrophage to sites of injury (Goncalves et al., 2010) and is present in high concentration in the macrophage nodules of rhesus monkeys with SIV encephalitis (Jagadish et al., 2012). While this might imply high CNS pGSN levels may be detrimental, several studies support the use of pGSN as a neuroprotective agent, for example in the treatment of Alzheimer's disease (Carro, 2010), multiple sclerosis (Kulakowska et al., 2010), and stroke (Le et al., 2011; Meisel et al., 2006; Zhang et al., 2011). Interestingly, in a primary cortical neuron model of ischemic neuronal injury, the enhanced expression of cGSN using the histone deacetylation inhibitor trichostatin A (TSA) was found to provide neuroprotection (Meisel et al., 2006), perhaps indicating a means for targeting the different isoforms for treatment. The mechanisms for these effects of GSN have yet to be definitively characterized.

GSN is known to be regulated by micromolar Ca^{2+}, among other factors, in its function of modulating filament disassembly of the actin cytoskeleton (Schafer and Cooper, 1995) as part of ion channel regulation, intracellular signaling, and apoptotic processes (Kwiatkowski, 1999). With regard to cell death, the presence of pGSN mitigates common features such as mitochondrial dysfunction, loss of membrane potential, and cytochrome C release (Harms et al., 2004). Perhaps relevant here, however, is evidence that pGSN may reduce the cytosolic Ca^{2+} overload resulting from exposure to excitotoxic stimuli by facilitating voltage-dependent Ca^{2+} channel (VDCC) and NMDA receptor channel rundown, while primary hippocampal neurons cultured from GSN-null mice and exposed to glutamate exhibited decreased actin filament depolymerization, increased Ca^{2+} influx, and amplified currents through VDCC and NMDA receptor channels (Endres et al., 1999; Furukawa et al., 1997). In one report, GSN even directly inhibited an HIV-1 viral protein (Vpr) from activating VDCC, thereby decreasing Ca^{2+} influx and reducing apoptosis (Qiao and McMillan, 2007). Despite what is known the altered concentration of pGSN in HAND and its anti-apoptotic effects, no research has been yet undertaken to explore the link between gp120-related neuronal damage, apoptotic Kv channel activity, and pGSN. While GSN has been found to oppose gp120-mediated actin remodeling (Garcia-Exposito et al., 2013), here we sought to determine concretely if pGSN might provide neuroprotective activity against gp120 exposure and to make clear the pathways involved. In addition, one report found the addition of GSN actually increased K^+ channel activity in human syncytiotrophoblasts (Montalbetti et al., 2005). In contrast, our results show that pGSN does indeed lessen apoptosis in cortical neurons exposed to gp120 (Fig. 1) by suppressing the gp120-associated upregulation of Kv2.1 expression (Fig. 7) and depolarizing shift of I_K inactivation properties (Fig. 6), thereby inhibiting gp120-enhanced I_K (Figs. 3 and 4) through Kv2.1 channels (Fig. 5), ultimately resulting in a reduction of gp120-induced Kv2.1-dependent apoptosis (Fig. 8). Considered with research conducted elsewhere and previously described, a tentative global picture emerges of the relationship between HIV-1 gp120 exposure, apoptotic K^+ efflux through Kv2.1 channels, and the protective role of pGSN in suppressing gp120-mediated enhancement of apoptotic Kv2.1 currents.

Although the present study demonstrates that pGSN protects gp120-induced neuronal injury via inhibition of gp120 enhancement of Kv2.1 expression and Kv2.1 current in rat cortical neuronal cultures, the exact mechanism underlying pGSN-mediated protection is not yet clear, nor is the site(s) of action – intracellular and/or extracellular? A previous study from our laboratory showed gp120 interacts with intracellular signaling, resulting in an enhancement of outward K^+ currents and consequent neuronal injury (Chen et al., 2011). In another study carried out on Jurkat T cells, GSN was found to block the interaction between viral protein and voltage-gated ion channels. These results suggest that pGSN may inhibit the interaction between gp120 and Kv2.1 leading to its neuroprotection. Another possibility is pGSN blocks the interaction between gp120 and Kv2.1 channel as viral proteins were found to interact with ion channels (Qiao and McMillan, 2007). In addition, pGSN may protect neurons through inhibition of gp120-mediated activation of caspases since gp120 has been shown to induce neuronal injury via activation of caspases (Louboutin et al., 2012; Tun et al., 2007) and GSN has been reported to, in complex with phosphatidylinositol 4, 5-biphosphate, inhibit caspase activity and retard apoptotic progression (Azuma et al., 2000). As to the site of pGSN action, it appears that pGSN acts extracellularly since pGSN inhibited gp120-induced shift of outward K^+ current inactivation curve shortly after brief bath perfusion of pGSN (Fig. 6). Nevertheless, further studies are definitely needed to unravel the mechanisms of pGSN-mediated neuroprotection and the site(s) of action.

It is worth pointing out that the effective concentrations for gp120 and GSN were different in studies measuring cell viability and K^+ current, with higher concentrations for studying cell viability. This is because, in the same time window, higher concentrations were needed

to produce changes in cell viability in comparison with the concentrations used to generate alterations of membrane ionic currents conducted by ion channels. Importantly, it is difficult to form gigaohm seal and record whole-cell current from injured cells. For these reasons, different concentrations of gp120 and GSN were employed in the present study.

In summarizing the present experiments, several principal findings bear mention. First, exposure to gp120 causes neuronal injury by amplifying neuronal I_K current via modification of Kv2.1 channel expression and activation. Second, the presence of pGSN mitigates gp120-induced apoptosis by inhibiting gp120-related enhancements of Kv2.1 channel activity. Collectively, these experimental results serve to further define the link between HAND pathogenesis and Kv channelopathies (Gelman et al., 2004), while at the same time supporting a potentially neuroprotective role for pGSN in the treatment of HAND and other neurodegenerative diseases.

Experimental Methods

Materials

HIV-1gp120 IIIB was purchased from Immunodiagnostics, Inc. (Woburn, MA). Aliquots of gp120 were kept as 100nM stock solution at −80°C. The stock solution was diluted to desired concentrations with artificial cerebrospinal fluid (ACSF) 2–5 min before test. Gelsolin (recombinant human plasma isoform) was purchased from Cytoskeleton, Inc (Denver, CO). All chemicals, unless otherwise specified, were from Sigma-Aldrich (St. Louis, MO).

Animals

Pregnant Sprague-Dawley rats were purchased from Charles River Laboratories (Wilmington, MA). Animals were housed at a constant temperature (22°C) and relative humidity (50%) under a regular light-dark cycle (light on at 7 AM and off at 5 PM) with free access to food and water. Animal use procedures were strictly reviewed by the Institutional Animal Care and Use Committee (IACUC) of the University of Nebraska Medical Center (IACUC No. 00-062-07).

Rat cortical neuron preparation and culture—Neurons were isolated from cortex tissue of E18 fetal Sprague-Dawley rats (Charles River Laboratories). Dissected tissue was then incubated with 0.25% trypsin and 200 U DNAase contained in Hank`s Buffered Salt Solution (HBSS) at 37°C for 15 min, and stop the digestion was stopped by addition of fetal bovine serum (FBS) at 10%. After centrifuging, the remaining tissue suspension was passed through nylon mesh with pore diameter size of 100 μm and 40 μm. Isolated cells were then suspended in neurobasal media (Gibco by Life Technologies) supplemented with 2% B27, 1% penicillin/streptomycin, 0.2% FBS, and 0.25 mM L-glutamine (Invitrogen by Life Technologies), and seeded either in 60 mm dishes at 2.5×10^6 cells/dish, 0.2×10^6 cells/well in 12 well plates containing 15 mm diameter coverslips, or in 48-well plates at 0.05×10^6 cells/well. All of the dishes, coverslips and plates were pre-coated with poly-D-lysine (1mg/ml). Cultures were maintained in supplemented neurobasal media for 8–12 days with half media change every 4 days. The purity of neuronal cells was determined to be >90% by staining with microtubule-associated protein-2 antibody (MAP-2: 1:1000, Chemicon International, Inc. Temecula, CA).

MTT and TUNEL assays—Cell viability was assessed by MTT assay. Pre-treated cells were exposed to 300μl of neurobasal media contained 500μg/ml 3-(4,5-dimethlthiazol-2-yl)-2,5-diphenyl tetrazolium bromide (MTT, Sigma-Aldrich) for 2 h at 37°C. MTT solution was then replaced with 300μl of dimethyl sphingosine (DMSO: Sigma-Aldrich) and shaking

the cells for 15min at 200 rpm for cell lysis. The optical density (OD) was measured at 560nm.

Neuronal apoptosis was evaluated using a Fluorescein *In Situ* Cell Death Detection Kit (Roche Applied Science, Indianapolis, IN). Briefly, Neurons grown on the poly-D-lysin-coated coverslips were fixed in 4% paraformaldehyde (PFA) for 1 h at room temperature and permeabilized in 0.1% Triton X-100 for 30 min. Neurons were then incubated in the TUNEL reaction mixture for 90 min at 37°. After washing, coverslips were mounted using vectashield mounting medium with DAPI (Vector Laboratories, Inc. Burlingame) and neurons were visualized via fluorescent microscope. The percentage of apoptotic neurons was determined based on TUNEL-positive cells normalized to DAPI-stained nuclei in 3 independent experiments.

Electrophysiology—Whole-cell recordings were made on neurons seeded on glass cover-slips at DIV 9–12. Recording electrodes, pulled from borosilicate glass micropipettes (WPI Inc. Sarasota, FL) with a P-97 micropipette puller (Sutter Instruments, Novato, CA), had a resistance of 5.0–8.0 MΩ when filled with intracellular solution contained (in mM): 120 K-gluconate, 10 KCl, 5 NaCl, 1 $CaCl_2$, 2 $MgCl_2$, 11 EGTA, 10 HEPES, 2 Mg-ATP and 1 GTP, adjusted pH to 7.3 with KOH. The extracellular solution was artificial cerebrospinal fluid (ACSF) contained (in mM) 140 NaCl, 5 KCl, 2.5 $CaCl_2$, 10 HEPES and 10 glucose, adjusted pH to 7.4 with NaOH. Tetrodotoxin (TTX, 1μM) and $CdCl_2$ (0.2 mM) were added to the ACSF to block voltage-gated Na^+ and Ca^{2+} channels, respectively. Stock solutions of 4-Aminopyridine (4-AP) and tetraethylammonium (TEA) were prepared in deionized water and diluted to working concentrations (4-AP 5mM, TEA 40mM) with ACSF in order to block A-type transient outward K^+ current (I_A) or delayed rectifier outward K^+ current (I_K). After establishment of the whole-cell patch configuration, the cells were allowed to stabilize for 3–5 min before tests. The recorded cells were held at −80 mV during voltage-clamping. Whole-cell outward K^+ currents were generated by voltage steps from the holding potential −80mV to +80mV in increments of 20mV. Current amplitudes were measured at the initial peak and at 300 ms and current densities (pA/pF) were calculated by dividing the amplitudes by the whole cell capacitance. Junction potential, pipette resistance were corrected and cell capacitance were compensated (∼70%). Current signals were filtered at 1 kHz and digitized at 5 kHz using Digidata 1440A digitizer (Molecular Devices). The current and voltage traces were displayed and recorded in a computer using Clampex 8.2 (Molecular Devices).

All experiments were done at room temperature (22–23°C). During experiments, the neuronal cultures were perfused with oxygenated (bubbled with 95% O_2 and 5% CO_2) ACSF at a constant flow rate of 2mL/min. The neuronal cells were identified by their morphology (triangular shaped) and their firing of action potentials in response to a depolarizing current impulse. Data were analyzed by Clampfit 8.2 (Molecular Devices) and graphed using Origin 8.5 (OriginLab, Northampton, MA). For bar graphs illustrating current densities, the instantaneous I_A and steady-state I_K generated by a voltage step from −80mV to +80mV were measured and the current density was then calculated by dividing the current and expressed as pA/pF.

RT-PCR—The total RNA isolation was completed with Trizol reagent (Invitrogen). RT-PCR was performed on 1–2 μg of the RNA sample with a SuperScript III first strand synthesis kit (Invitrogen) using the oligo-dT primers. The resulting cDNA was then used for PCR amplification. Primer sequences for Kv1.1 were forward GGAGCGCCCCCTACCCGAGAAG, reverse GGTGAATGGTGCCCGTGAAGTCCT, product length 191 base pairs (bp); for Kv2.1, forward TGGAGAAGCCCAACTCATC, reverse CAATGGTGGAGAGGACATG, product length 78bp; for Kv4.2, forward GCCGCAGCGCCTAGTCGTTACC, reverse

TGATAGCCATTGTGAGGGAAAAGAGCA, product length 262 bp; and for GAPDH, forward TCAAGAAGGTGGTGAAGCAG, reverse AGGTGGAAGAATGGGAGTTG, product length 126 bp. PCR cycles were performed as follows: initial 5 min at 95°C, then 30 cycles of 95°C (15 s), 55°C (30 s), and 72°C (45 s), followed by 10 min at 72°C for further extension.

Immunoblotting—Western blots were performed using standard protocol. Briefly, pre-treated neurons were washed twice with ice-cold PBS and total proteins were extracted using RIPA (Sigma- Aldrich). BCA protein assay kit (Thermo, US) was then employed to quantify protein. Fifteen microgram proteins were separated by electrophoresis using 10% SDS-polyacrylamide gels and transferred to nitrocellulose polyvinylidene difluoried (PVDF) membranes. Following transferring, PVDF membranes were blocked with 5% non-fat milk in Tris-Buffered Saline (TBS) (all products from Bio-Rad Laboratories, Hercules, CA). Membranes were probed overnight at 4°C with primary antibodies including rabbit polyclonal $K_v1.1$ (1.500), mouse monoclonal $K_v2.1$,(1:500) (Abcam Inc. Cambridge, MA), rabbit anti-Kv4.2 (1:200, CHENICON International, Inc.), anti-mouse β-actin (1:5,000), or anti-rabbit GAPDH (1:5,000) to detect Kv1.1, Kv2.1, Kv4.2, GAPDH, and β-actin protein. Afterwards, membranes were washed in TBS with 0.2% Tween (TBS-T) and incubated with either HRP-conjugated onto rabbit or anti-mouse secondary antibody (1:10,000, Haacson ImmunoResearch Laboratories, West Grove, PA) for 1 h at room temperature. Finally, membranes were washed and visualized by Pierce ECL Western Blotting Substrate (Thermo Scientific, Rockford, IL). Band densities captured by ImageJ.

Statistical analyses

All data were expressed as mean ± S.E.M. unless otherwise indicated. Statistical analyses were performed by one-way ANOVA or two-tailed *t* test. The difference between groups was considered significant when $p<0.05$.

Acknowledgments

References

Anderson E, Zink W, Xiong H, Gendelman HE. HIV-1-associated dementia: a metabolic encephalopathy perpetrated by virus-infected and immune-competent mononuclear phagocytes. J Acquir Immune Defic Syndr. 2002; 31(Suppl 2):S43–S54. [PubMed: 12394782]

Azuma T, Koths K, Flanagan L, Kwiatkowski D. Gelsolin in complex with phosphatidylinositol 4,5-bisphosphate inhibits caspase-3 and −9 to retard apoptotic progression. J Biol Chem. 2000; 275:3761–3766. [PubMed: 10660524]

Bucki R, Levental I, Kulakowska A, Janmey PA. Plasma gelsolin: function, prognostic value, and potential therapeutic use. Curr Protein Pept Sci. 2008; 9:541–551. [PubMed: 19075745]

Carro E. Gelsolin as therapeutic target in Alzheimer's disease. Expert Opin Ther Targets. 2010; 14:585–592. [PubMed: 20433353]

Catani MV, Corasaniti MT, Navarra M, Nistico G, Finazzi-Agro A, Melino G. gp120 induces cell death in human neuroblastoma cells through the CXCR4 and CCR5 chemokine receptors. J Neurochem. 2000; 74:2373–2379. [PubMed: 10820198]

Chen L, Liu J, Xu C, Keblesh J, Zang W, Xiong H. HIV-1gp120 induces neuronal apoptosis through enhancement of 4-aminopyridine-senstive outward K+ currents. PloS one. 2011; 6:e25994. [PubMed: 22016798]

Endres M, Fink K, Zhu J, Stagliano NE, Bondada V, Geddes JW, Azuma T, Mattson MP, Kwiatkowski DJ, Moskowitz MA. Neuroprotective effects of gelsolin during murine stroke. J Clin Invest. 1999; 103:347–354. [PubMed: 9927495]

Furukawa K, Fu W, Li Y, Witke W, Kwiatkowski DJ, Mattson MP. The actin-severing protein gelsolin modulates calcium channel and NMDA receptor activities and vulnerability to excitotoxicity in hippocampal neurons. J Neurosci. 1997; 17:8178–8186. [PubMed: 9334393]

Garcia-Exposito L, Ziglio S, Barroso-Gonzalez J, de Armas-Rillo L, Valera MS, Zipeto D, Machado JD, Valenzuela-Fernandez A. Gelsolin activity controls efficient early HIV-1 infection. Retrovirology. 2013; 10:39. [PubMed: 23575248]

Gelman BB, Soukup VM, Schuenke KW, Keherly MJ, Holzer C 3rd, Richey FJ, Lahart CJ. Acquired neuronal channelopathies in HIV-associated dementia. J Neuroimmunol. 2004; 157:111–119. [PubMed: 15579287]

Gendelman, HE.; Eiden, L.; Epstein, L.; Grant, I.; Lipton, S.; McArthur, J.; Pomerantz, R.; Price, R.; Swindells, S. The Neuropathogenesis of HIV-1-Dementia: APanel Discussion. In: Gendelman, HE.; Lipton, SA.; Epstein, LG.; Swindells, S., editors. The neurology of AIDS. 1 ed.. New York: Chapman and Hall; 1998. p. 1-10.

Goncalves AF, Dias NG, Moransard M, Correia R, Pereira JA, Witke W, Suter U, Relvas JB. Gelsolin is required for macrophage recruitment during remyelination of the peripheral nervous system. Glia. 2010; 58:706–715. [PubMed: 20014276]

Harms C, Bosel J, Lautenschlager M, Harms U, Braun JS, Hortnagl H, Dirnagl U, Kwiatkowski DJ, Fink K, Endres M. Neuronal gelsolin prevents apoptosis by enhancing actin depolymerization. Molecular and cellular neurosciences. 2004; 25:69–82. [PubMed: 14962741]

Haverland N, Pottiez G, Wiederin J, Ciborowski P. Immunoreactivity of anti-gelsolin antibodies: implications for biomarker validation. J Transl Med. 2010; 8:137. [PubMed: 21171974]

Heaton RK, Clifford DB, Franklin DR Jr. Woods SP, Ake C, Vaida F, Ellis RJ, Letendre SL, Marcotte TD, Atkinson JH, Rivera-Mindt M, Vigil OR, Taylor MJ, Collier AC, Marra CM, Gelman BB, McArthur JC, Morgello S, Simpson DM, McCutchan JA, Abramson I, Gamst A, Fennema-Notestine C, Jernigan TL, Wong J, Grant I. HIV-associated neurocognitive disorders persist in the era of potent antiretroviral therapy: CHARTER Study. Neurology. 2010; 75:2087–2096. [PubMed: 21135382]

Herrington J. Gating modifier peptides as probes of pancreatic beta-cell physiology. Toxicon. 2007; 49:231–238. [PubMed: 17101164]

Hu CL, Zeng XM, Zhou MH, Shi YT, Cao H, Mei YA. Kv 1.1 is associated with neuronal apoptosis and modulated by protein kinase C in the rat cerebellar granule cell. J Neurochem. 2008; 106:1125–1137. [PubMed: 18466331]

Hu D, Liu J, Xiong H. Enhancement of neuronal outward delayed rectifier K+ current by human monocyte-derived macrophages. Glia. 2009; 57:1492–1500. [PubMed: 19306367]

Jagadish T, Pottiez G, Fox HS, Ciborowski P. Plasma gelsolin accumulates in macrophage nodules in brains of simian immunodeficiency virus infected rhesus macaques. J Neurovirol. 2012; 18:113–119. [PubMed: 22403026]

Kaul M, Garden GA, Lipton SA. Pathways to neuronal injury and apoptosis in HIV-associated dementia. Nature. 2001; 410:988–994. [PubMed: 11309629]

Kaul M, Lipton SA. Mechanisms of neuroimmunity and neurodegeneration associated with HIV-1 infection and AIDS. J Neuroimmune Pharmacol. 2006a; 1:138–151. [PubMed: 18040780]

Kaul M, Lipton SA. Mechanisms of neuronal injury and death in HIV-1 associated dementia. Curr HIV Res. 2006b; 4:307–318. [PubMed: 16842083]

Keblesh J, Hu D, Xiong H. Voltage-gated potassium channels in human immunodeficiency virus type-1 (HIV-1)-associated neurocognitive disorders. J Neuroimmune Pharmacol. 2009a; 4:60–70. [PubMed: 18459047]

Keblesh JP, Dou H, Gendelman HE, Xiong H. 4-Aminopyridine improves spatial memory in a murine model of HIV-1 encephalitis. J Neuroimmune Pharmacol. 2009b; 4:317–327. [PubMed: 19462247]

Kranick SM, Nath A. Neurologic complications of HIV-1 infection and its treatment in the era of antiretroviral therapy. Continuum (Minneap Minn). 2012; 18:1319–1337. [PubMed: 23221843]

Kulakowska A, Ciccarelli NJ, Wen Q, Mroczko B, Drozdowski W, Szmitkowski M, Janmey PA, Bucki R. Hypogelsolinemia, a disorder of the extracellular actin scavenger system, in patients with multiple sclerosis. BMC Neurol. 2010; 10:107. [PubMed: 21040581]

Kulakowska A, Drozdowski W, Sadzynski A, Bucki R, Janmey PA. Gelsolin concentration in cerebrospinal fluid from patients with multiple sclerosis and other neurological disorders. Eur J Neurol. 2008; 15:584–588. [PubMed: 18474076]

Kwiatkowski DJ. Functions of gelsolin: motility, signaling, apoptosis, cancer. Curr Opin Cell Biol. 1999; 11:103–108. [PubMed: 10047530]

Kwiatkowski DJ, Stossel TP, Orkin SH, Mole JE, Colten HR, Yin HL. Plasma and cytoplasmic gelsolins are encoded by a single gene and contain a duplicated actin-binding domain. Nature. 1986; 323:455–458. [PubMed: 3020431]

Kwiatkowski DJ, Westbrook CA, Bruns GA, Morton CC. Localization of gelsolin proximal to ABL on chromosome 9. Am J Hum Genet. 1988; 42:565–572. [PubMed: 2831714]

Le HT, Hirko AC, Thinschmidt JS, Grant M, Li Z, Peris J, King MA, Hughes JA, Song S. The protective effects of plasma gelsolin on stroke outcome in rats. Exp Transl Stroke Med. 2011; 3:13. [PubMed: 22047744]

Lee S, Milescu M, Jung HH, Lee JY, Bae CH, Lee CW, Kim HH, Swartz KJ, Kim JI. Solution structure of GxTX-1E, a high-affinity tarantula toxin interacting with voltage sensors in Kv2.1 potassium channels. Biochemistry. 2010; 49:5134–5142. [PubMed: 20509680]

Lei Z, Deng P, Li Y, Xu ZC. Downregulation of Kv4.2 channels mediated by NR2B–containing NMDA receptors in cultured hippocampal neurons. Neuroscience. 2010; 165:350–362. [PubMed: 19857555]

Lipton SA, Gendelman HE. Dementia associated with the acquired immunodeficiency syndrome. N. Engl. J. Med. 1995; 332:934–940. [PubMed: 7877652]

Louboutin JP, Agrawal L, Reyes BA, van Bockstaele EJ, Strayer DS. Gene delivery of antioxidant enzymes inhibits human immunodeficiency virus type 1 gp120-induced expression of caspases. Neuroscience. 2012; 214:68–77. [PubMed: 22531373]

Mattson MP, Haughey NJ, Nath A. Cell death in HIV dementia. Cell Death Differ. 2005; 12(Supp l): 893–904. [PubMed: 15761472]

McArthur J, Smith B. Neurologic Complications and Considerations in HIV-Infected Persons. Curr Infect Dis Rep. 2013; 15:61–66. [PubMed: 23307491]

Meisel A, Harms C, Yildirim F, Bosel J, Kronenberg G, Harms U, Fink KB, Endres M. Inhibition of histone deacetylation protects wild-type but not gelsolin-deficient neurons from oxygen/glucose deprivation. J Neurochem. 2006; 98:1019–1031. [PubMed: 16895577]

Meucci O, Miller RJ. gp120-induced neurotoxicity in hippocampal pyramidal neuron cultures: protective action of TGF-beta1. J Neurosci. 1996; 16:4080–4088. [PubMed: 8753870]

Misonou H, Mohapatra DP, Park EW, Leung V, Zhen D, Misonou K, Anderson AE, Trimmer JS. Regulation of ion channel localization and phosphorylation by neuronal activity. Nat Neurosci. 2004; 7:711–718. [PubMed: 15195093]

Montalbetti N, Li Q, Timpanaro GA, Gonzalez-Perrett S, Dai XQ, Chen XZ, Cantiello HF. Cytoskeletal regulation of calcium-permeable cation channels in the human syncytiotrophoblast: role of gelsolin. J Physiol. 2005; 566:309–325. [PubMed: 15845576]

Mothobi NZ, Brew BJ. Neurocognitive dysfunction in the highly active antiretroviral therapy era. Curr Opin Infect Dis. 2012; 25:4–9. [PubMed: 22156897]

Muller WE, Schroder HC, Ushijima H, Dapper J, Bormann J. gp120 of HIV-1 induces apoptosis in rat cortical cell cultures: prevention by memantine. Eur J Pharmacol. 1992; 226:209–214. [PubMed: 1426020]

Murakoshi H, Trimmer JS. Identification of the Kv2.1 K+ channel as a major component of the delayed rectifier K+ current in rat hippocampal neurons. J Neurosci. 1999; 19:1728–1735. [PubMed: 10024359]

Nath A, Geiger J. Neurobiological aspects of human immunodeficiency virus infection: neurotoxic mechanisms. Prog Neurobiol. 1998; 54:19–33. [PubMed: 9460791]

Nath A, Haughey NJ, Jones M, Anderson C, Bell JE, Geiger JD. Synergistic neurotoxicity by human immunodeficiency virus proteins Tat and gp120: protection by memantine. Ann Neurol. 2000; 47:186–194. [PubMed: 10665489]

Pal S, Hartnett KA, Nerbonne JM, Levitan ES, Aizenman E. Mediation of neuronal apoptosis by Kv2.1-encoded potassium channels. J Neurosci. 2003; 23:4798–4802. [PubMed: 12832499]

Pal SK, Takimoto K, Aizenman E, Levitan ES. Apoptotic surface delivery of K+ channels. Cell Death Differ. 2006; 13:661–667. [PubMed: 16273079]

Pannaccione A, Boscia F, Scorziello A, Adornetto A, Castaldo P, Sirabella R, Taglialatela M, Di Renzo GF, Annunziato L. Up-regulation and increased activity of KV3.4 channels and their accessory subunit MinK-related peptide 2 induced by amyloid peptide are involved in apoptotic neuronal death. Mol Pharmacol. 2007; 72:665–673. [PubMed: 17495071]

Peng X, Zhang X, Wang L, Zhu Q, Luo J, Wang W, Wang X. Gelsolin in cerebrospinal fluid as a potential biomarker of epilepsy. Neurochem Res. 2011; 36:2250–2258. [PubMed: 21786170]

Pieri M, Amadoro G, Carunchio I, Ciotti MT, Quaresima S, Florenzano F, Calissano P, Possenti R, Zona C, Severini C. SP protects cerebellar granule cells against beta-amyloid-induced apoptosis by down-regulation and reduced activity of Kv4 potassium channels. Neuropharmacology. 2010; 58:268–276. [PubMed: 19576909]

Potter MC, Figuera-Losada M, Rojas C, Slusher BS. Targeting the Glutamatergic System for the Treatment of HIV-Associated Neurocognitive Disorders. J Neuroimmune Pharmacol. 2013; 8:594–607. [PubMed: 23553365]

Pottiez G, Haverland N, Ciborowski P. Mass spectrometric characterization of gelsolin isoforms. Rapid Commun Mass Spectrom. 2010; 24:2620–2624. [PubMed: 20740538]

Qiao H, McMillan JR. Gelsolin segment 5 inhibits HIV-induced T-cell apoptosis via Vpr-binding to VDAC. FEBS Lett. 2007; 581:535–540. [PubMed: 17254575]

Remillard CV, Yuan JX. Activation of K+ channels: an essential pathway in programmed cell death. Am J Physiol Lung Cell Mol Physiol. 2004; 286:L49–L67. [PubMed: 14656699]

Rozek W, Ricardo-Dukelow M, Holloway S, Gendelman HE, Wojna V, Melendez LM, Ciborowski P. Cerebrospinal fluid proteomic profiling of HIV-1-infected patients with cognitive impairment. J Proteome Res. 2007; 6:4189–4199. [PubMed: 17929958]

Schafer DA, Cooper JA. Control of actin assembly at filament ends. Annu Rev Cell Dev Biol. 1995; 11:497–518. [PubMed: 8689567]

Shen QJ, Zhao YM, Cao DX, Wang XL. Contribution of Kv channel subunits to glutamate-induced apoptosis in cultured rat hippocampal neurons. J Neurosci Res. 2009; 87:3153–3160. [PubMed: 19472219]

Tun C, Guo W, Nguyen H, Yun B, Libby RT, Morrison RS, Garden GA. Activation of the extrinsic caspase pathway in cultured cortical neurons requires p53-mediated down-regulation of the X-linked inhibitor of apoptosis protein to induce apoptosis. J Neurochem. 2007; 102:1206–1219. [PubMed: 17488272]

Wiederin J, Rozek W, Duan F, Ciborowski P. Biomarkers of HIV-1 associated dementia: proteomic investigation of sera. Proteome Sci. 2009; 7:8. [PubMed: 19292902]

Wu P, Price P, Du B, Hatch WC, Terwilliger EF. Direct cytotoxicity of HIV-1 envelope protein gp120 on human NT neurons. Neuroreport. 1996; 7:1045–1049. [PubMed: 8804048]

Xiong H, Zeng YC, Lewis T, Zheng J, Persidsky Y, Gendelman HE. HIV-1 infected mononuclear phagocyte secretory products affect neuronal physiology leading to cellular demise: relevance for HIV-1-associated dementia. J Neurovirol. 2000; 6(Suppl 1):S14–S23. [PubMed: 10871761]

Yin HL, Kwiatkowski DJ, Mole JE, Cole FS. Structure and biosynthesis of cytoplasmic and secreted variants of gelsolin. J Biol Chem. 1984; 259:5271–5276. [PubMed: 6325429]

Yu SP. Regulation and critical role of potassium homeostasis in apoptosis. Prog Neurobiol. 2003; 70:363–386. [PubMed: 12963093]

Yu SP, Yeh CH, Sensi SL, Gwag BJ, Canzoniero LM, Farhangrazi ZS, Ying HS, Tian M, Dugan LL, Choi DW. Mediation of neuronal apoptosis by enhancement of outward potassium current. Science. 1997; 278:114–117. [PubMed: 9311914]

Zhang QH, Chen Q, Kang JR, Liu C, Dong N, Zhu XM, Sheng ZY, Yao YM. Treatment with gelsolin reduces brain inflammation and apoptotic signaling in mice following thermal injury. J Neuroinflammation. 2011; 8:118. [PubMed: 21936896]
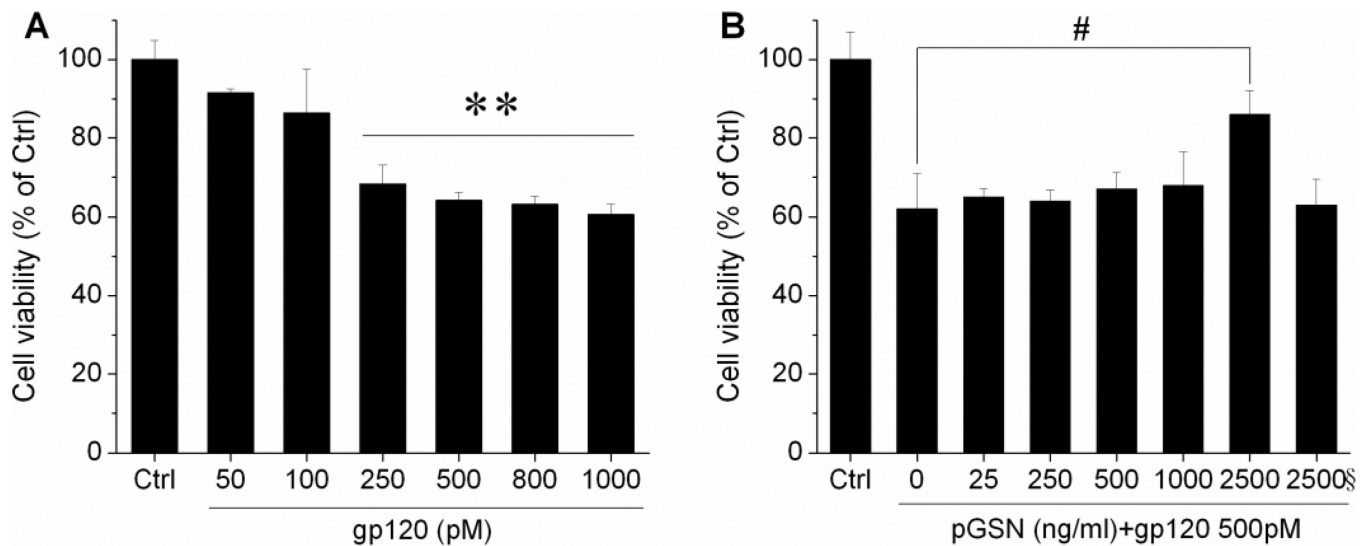
Figure 1. pGSN protection of gp120-induced neuronal damage
(**A**) Dose-dependent toxicity of gp120 on cortical neurons. Exposure of neuronal cells to gp120 at and greater than 500pM resulted in maximal reduction in cell viability. (**B**) Neurons were treated with 500 pM gp120 and different concentrations of GSN for 24 h. pGSN significantly protected neurons from gp120-mediated damage at a concentration of 2.5 μg/ml. Heat (boiled) inactivated pGSN (indicated by a symbol §, the same as in other figures) failed to produce protective effect. Data represent mean ± SEM from at least 5 independent experiments and expressed as % of control. ** p <0.01 vs. control; # p<0.05 vs. gp120 (0 GSN).
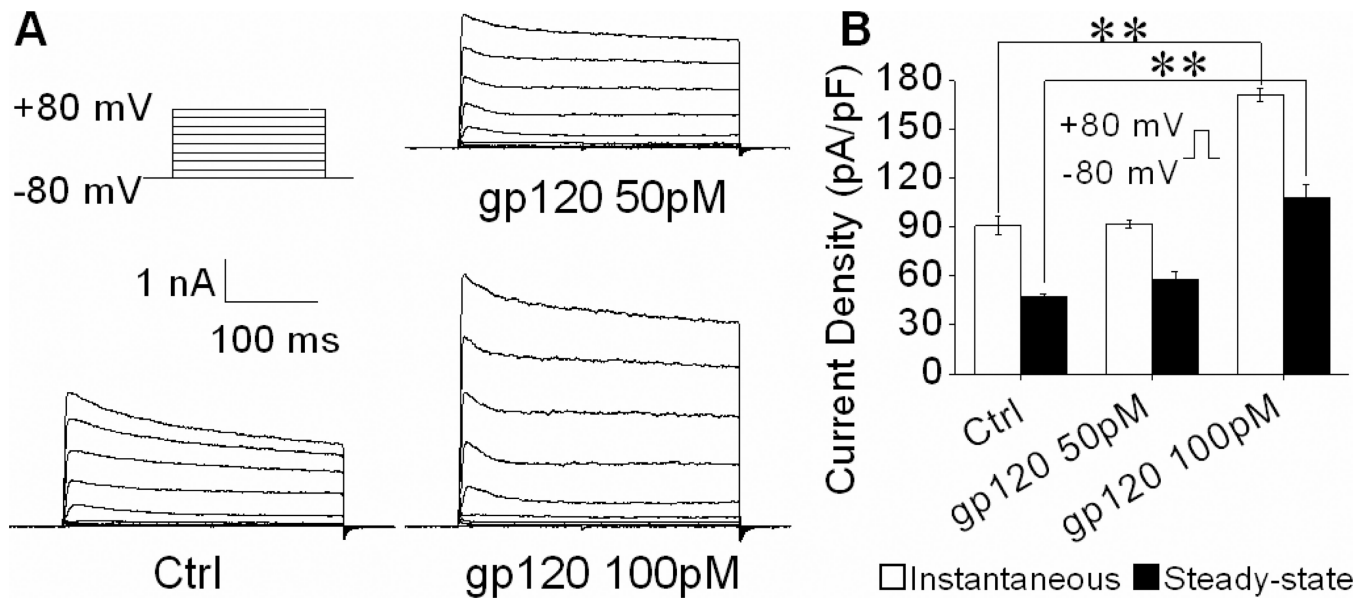
Figure 2. Gp120 increases outward K⁺ currents

Cultures were treated without or with 50pM, 100pM gp120 respectively 24h. (**A**) Representative current traces evoked by voltage protocol (upper left, not proportional to the current traces in duration) from three different neurons treated without (Ctrl) or with 50pM, 100pM gp120 respectively for 24h. Note gp120 at 100pM increased outward K⁺ currents. (**B**) Instantaneous and steady-state current densities measured at +80mV from groups of neurons treated without (Ctrl, n=15) or with 50pM gp120 (n=13), 100pM gp120 (n=18). Note that gp120 increased both instantaneous and steady-state outward K⁺ currents at 100 pM. ** p<0.01 vs. control.
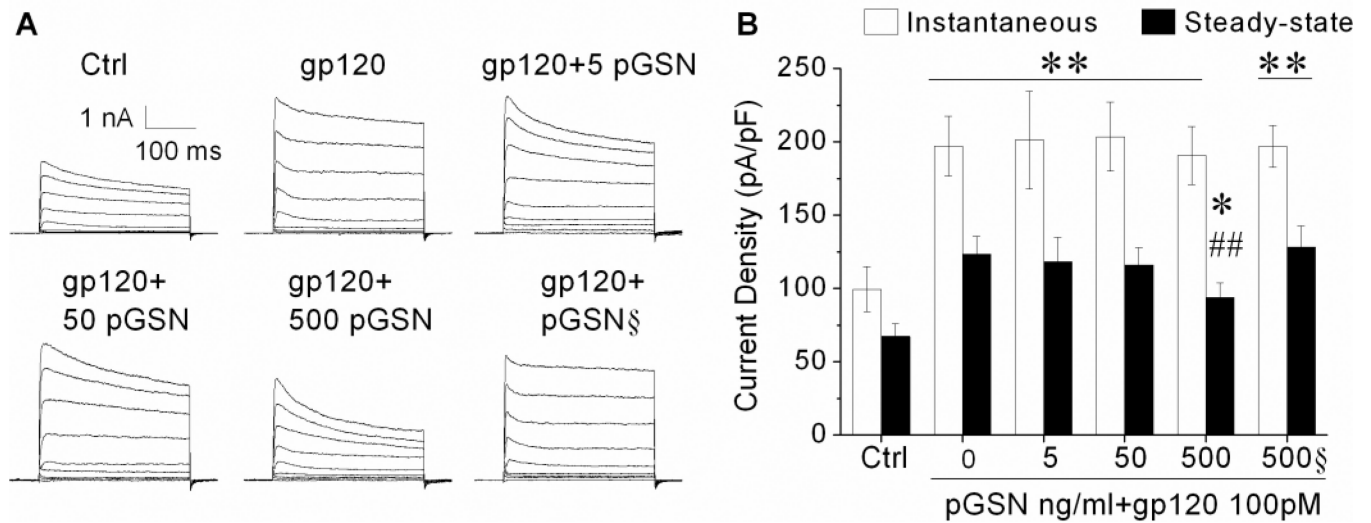
Figure 3. pGSN decrease of gp120 enhancement of neuronal outward K+ currents
(**A**) Representative current traces recorded from 6 different neurons treated with gp120 (100pM) alone, or gp120 (100pM) and different concentrations of pGSN (5, 50, 500, 500§), or untreated control. Whole-cell currents were generated by voltage steps from the holding potential of −80mV to +80mV in increments of 20mV. Both instantaneous and steady-state outward K$^+$ currents were measured and current densities were calculated and displayed in (**B**). pGSN only inhibited gp120-induced steady-state K$^+$ current. In contrast, heat denatured pGSN lose such an inhibitory ability. * $p < 0.05$ vs. control, ** $p < 0.01$ vs. control; ## $p < 0.01$ vs. gp120 alone.
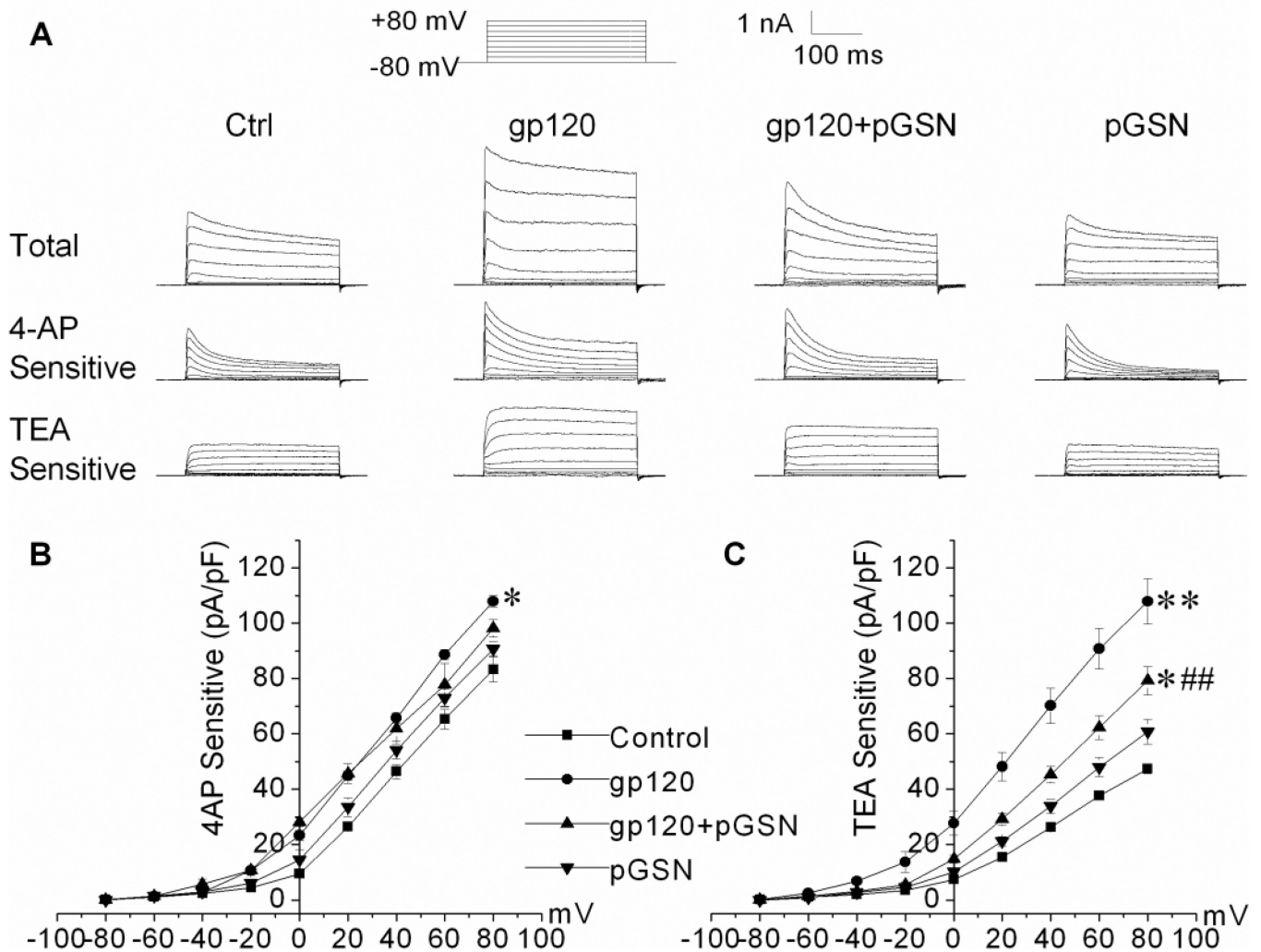
Figure 4. pGSN inhibits gp120 enhancement of TEA-sensitive I_K, but not 4-AP-sensitive I_A
(**A**) shows representative total (upper), 4-AP-sensitive (middle) and TEA-sensitive (lower) outward K^+ currents recorded from neurons treated with gp120 (100pM), gp120 (100pM) +pGSN(500ng/ml), pGSN (500ng/ml) or untreated controls(Ctrl). (**B**) and (**C**) are current density-voltage relationships, illustrating GSN inhibition of TEA-sensitive I_K. pGSN alone did not affect either the 4-AP- or TEA-sensitive outward K^+ currents (p>0.05). For each type of outward K^+ currents, 25 neurons were recorded in each treatment group. * p<0.05 vs. control, ** p<0.01 vs. control; ## p<0.01 vs. gp120 group.
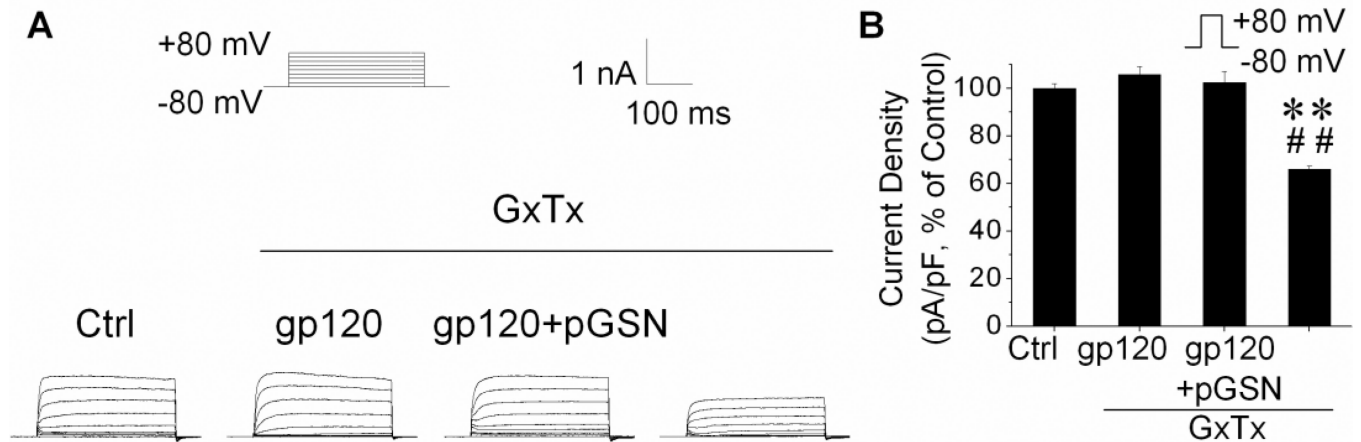
Figure 5. Involvement of Kv2.1 in pGSN inhibition of gp120 enhancement of TEA-sensitive I_K
Cultures were treated for 24 h with 100 pM gp120, 500 ng/ml pGSN or gp120 and pGSN.
(**A**) Representative TEA sensitive currents recorded from neurons with treatments indicated.
TEA sensitive I_K was recorded in the presence of 4-AP (5mM) alone or 4-AP and GxTx
(50nM). Note that GxTx, a specific Kv2.1 channel blocker, abolished pGP120 enhancement
of the TEA sensitive I_K. (**B**) a summary bar graph of current densities (n=25) showing GxTx
inhibition of gp120 increase of TEA sensitive K^+ currents generated by a voltage step from
−80 to +80mV and GxTx per se decreased TEA sensitive K^+ currents. **$p<0.01$ vs.
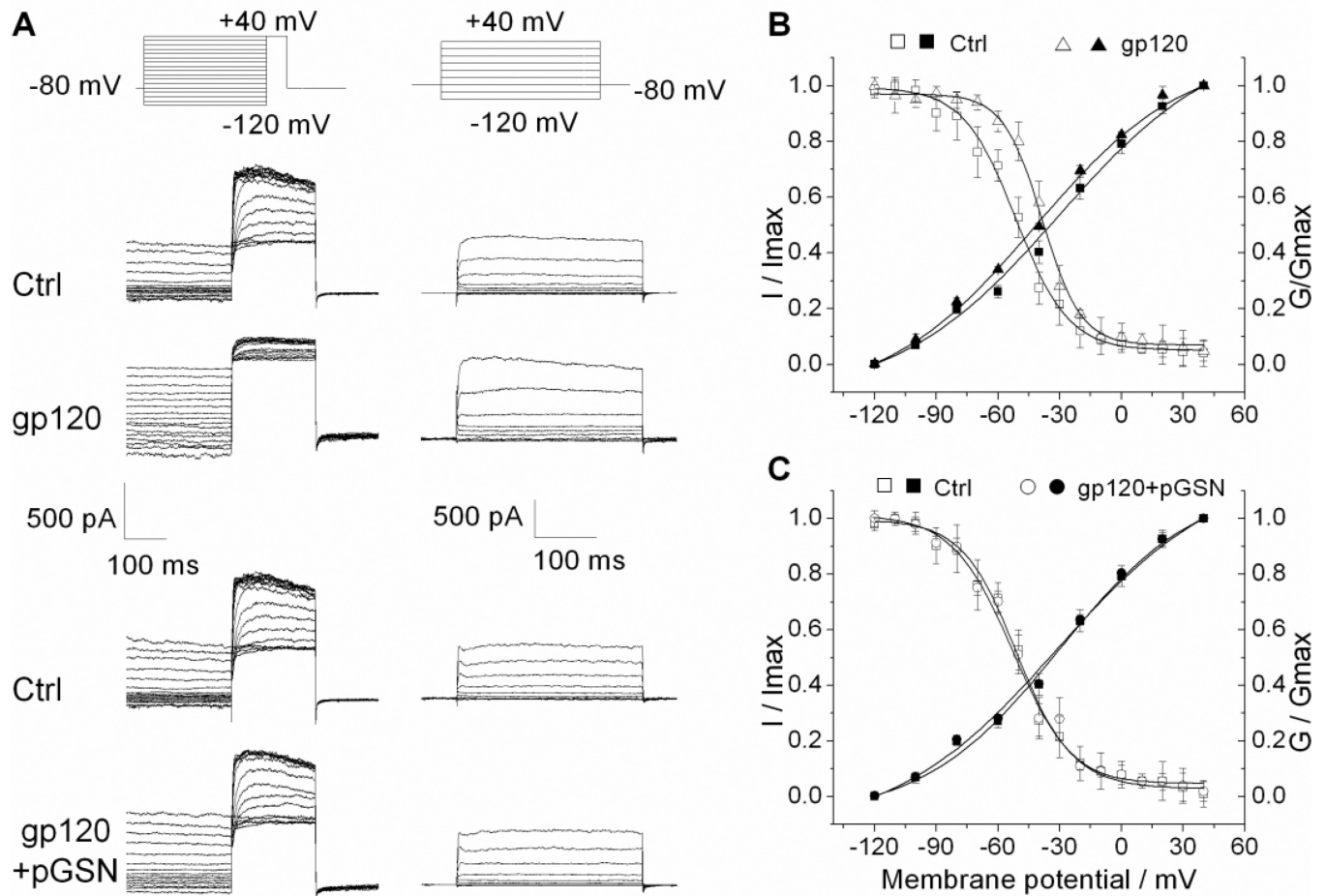control; ##$p<0.01$ vs. gp120 group.

Figure 6. pGSN blocks gp120-induced shift of TEA sensitive K$^+$ current inactivation curve
(**A**) The original current traces generated by inactivation and activation voltage protocols
(upper) before and after bath perfusion of 200 pM gp120 (middle) or 200 pM gp120 and 1
µg/ml pGSN (lower) from two different neurons. Normalized data points were fitted with
the Boltzmann equation: $I/I_{max}=1/\{1+\exp[(V-V_{1/2})/k]\}$ and $G/G_{max}=1-1/\{1+\exp[(V-V_{1/2})]/k\}$. Each point represents the mean ± SEM, n=5. For inactivation, $V_{1/2}$ was −38.51 mV in
the presence of gp120 compared with −51.64 mV in Control (**B**). $V_{1/2}$ was −52.61 mV for
gp120+GSN compared with −51.14 mV for Control (**C**). For activation, $V_{1/2}$ values for
TEA sensitive K$^+$ currents were −41.93 mV in the presence of gp120 vs −30.59mV in
Control (**B**); and −31.13 mV in gp120+GSN group vs −30.32 mV in Control group (**C**).
These results showed that gp120 shifted inactivation curve to the right, which was inhibited
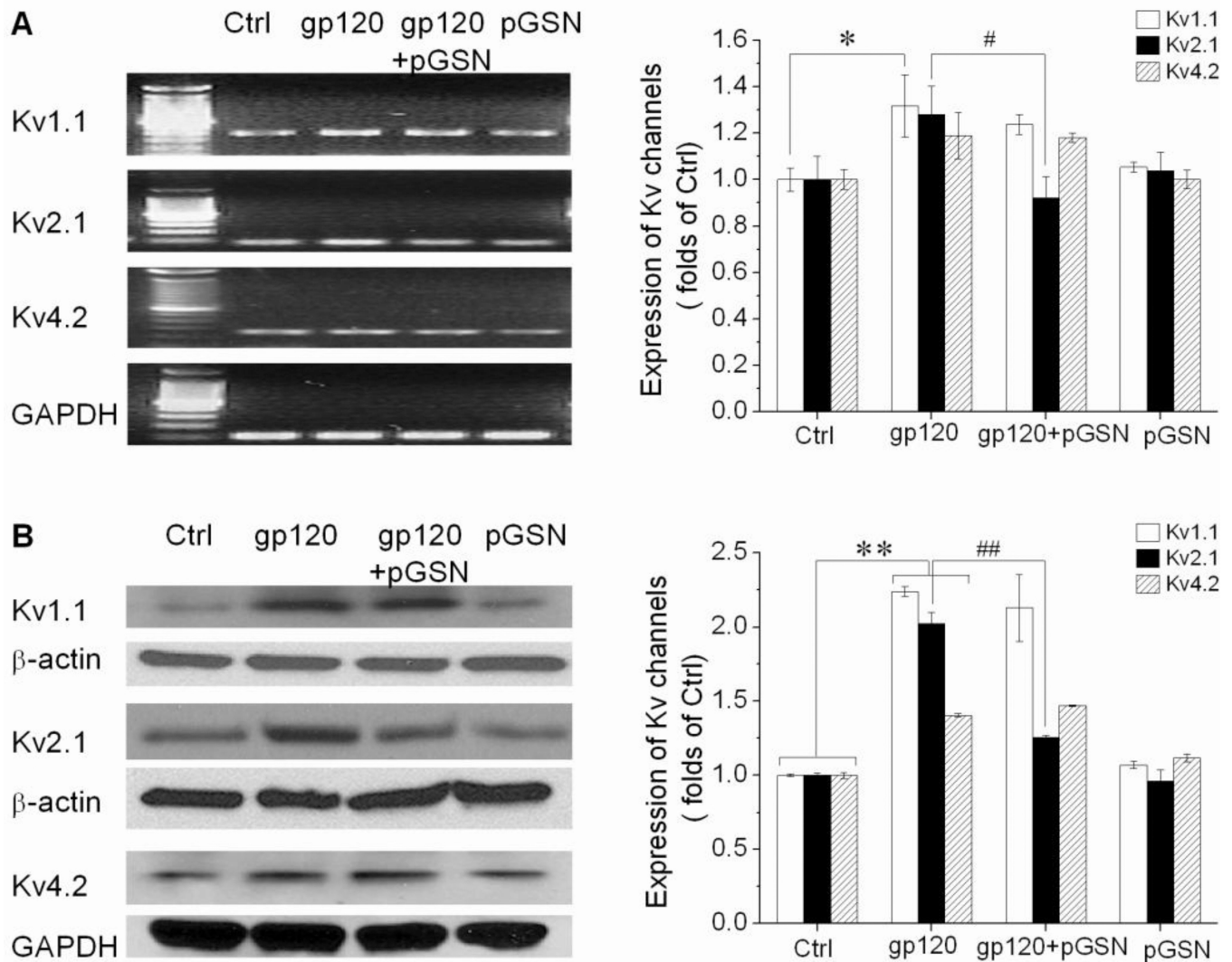by pGSN.

Figure 7. Inhibition of gp120-induced Kv2.1 channel expression by pGSN
Neuronal cultures were treated with 500 pM gp120 with or without 2.5μg/ml pGSN for 24h. Band density was analyzed by Image J and normalized by internal control. Data represents means ± SEM from 3 independent experiments. (**A**) gp120 increased the levels of Kv1.1 mRNA expression (p<0.05). Although increased levels of Kv2.1 and Kv4.2 mRNA expression did not reach the statistical significance (p>0.05 compare to control), the expression levels of Kv2.1 mRNA was down-regulated by pGSN compared to gp120 group (p<0.05). (**B**) gp120 significantly increased the levels of Kv1.1, Kv2.1 and Kv4.2 channel protein expression (p<0.01). pGSN significantly reduced only Kv2.1 channel protein expression (p<0.01). pGSN alone did not alter the expression levels of Kv channels. * p< 0.05 vs. control; **p<0.01 vs. control; #p<0.05 vs. gp120 group; ##P<0.01 vs. gp120 group.
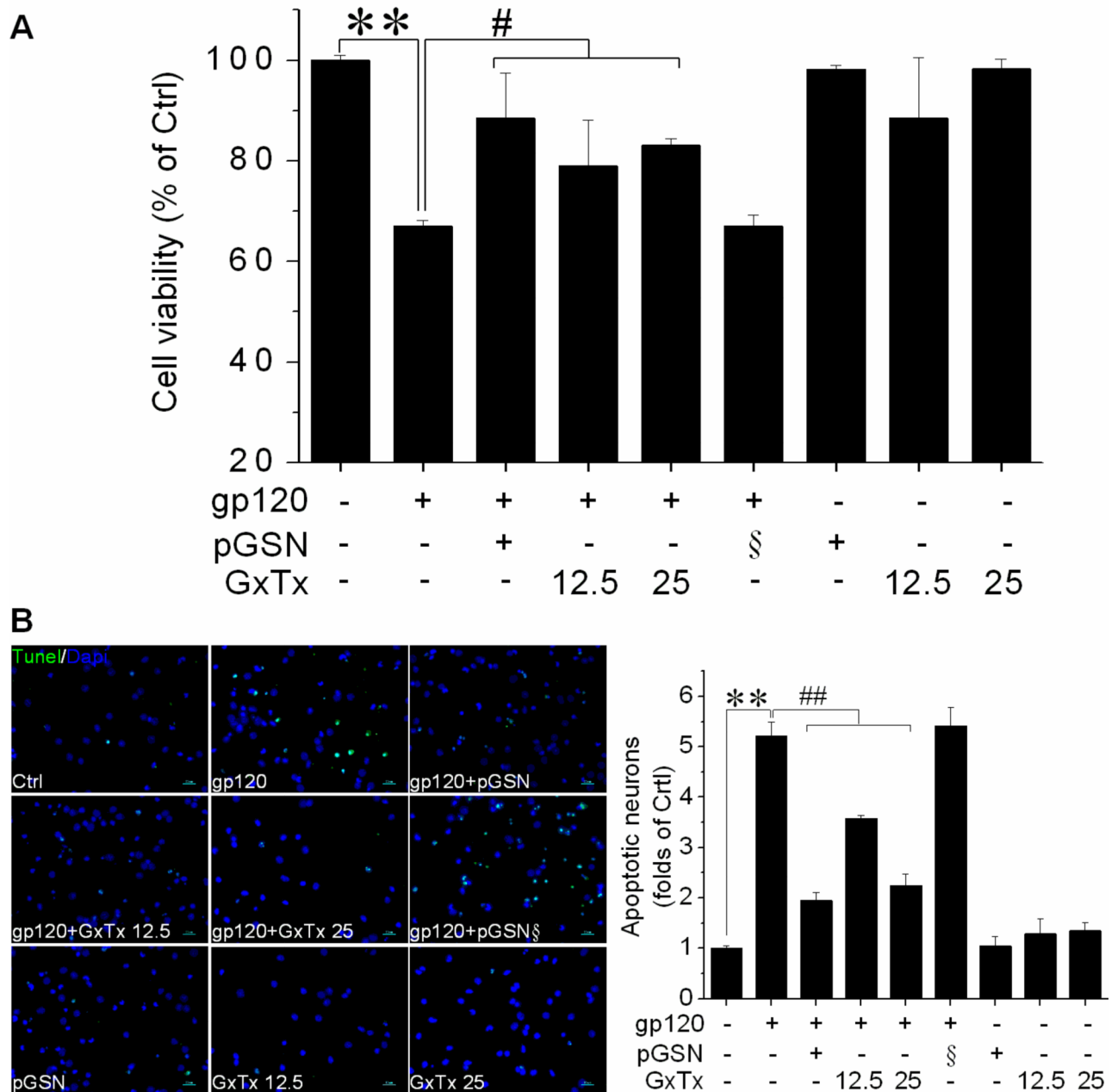
Figure 8. pGSN protects against gp120-induced neuronal damage via Kv2.1
Neurons were exposed to gp120 (500pM), pGSN (2.5μg/ml), gp120(500pM) and pGSN
(2.5μg/ml), or heat-inactivated pGSN (2.5μg/ml) in the presence or absence co-incubated
GxTx (12.5 or 25 nM) for 24h. (**A**) Cell viability determined by MTT assay exhibited that
gp120 exposure reduced cell viability (p<0.01 compare to Control), which was attenuated by
GSN or GxTx. Heat-inactivated pGSN (§) showed no protective effect. pGSN or GxTx
alone did not alter cell viability. (**B**) left panel shows TUNEL staining results as a measure
of apoptosis, with cell nuclei visualized using Dapi stain. 10 visual fields were analyzed for
each of three independent experiments. Gp120 induced neuronal apoptosis that was

attenuated by either pGSN or GxTx. These data suggest that pGSN protects against gp120-induced neuronal damage via Kv2.1. **$p<0.01$ vs. control; #$p<0.05$ vs. gp120 group; ## $p<0.01$ vs. gp120 group. Scale bars denote 50μm.